

## Response of the sapphire to low velocity impact

J.Buchar<sup>1</sup>, J.Trnka<sup>2</sup>, R.Řídký<sup>3</sup>

<sup>1</sup>Mendel University, Zemedelska 1, 613 00 Brno, Czech Republic

<sup>2</sup>Institute of Thermomechanics the Czech Academy of Sciences, Dolejskova 5, 182 00 Prague, Czech Republic

<sup>3</sup>SVS FEM Ltd. Trnkova 117c, 628 00 Brno, Czech Republic

---

**ABSTRACT:** Sapphire specimens in form of cylinder (5 mm in diameter and 25 mm in length) were launched against a steel bar which was instrumented with strain gauges to measure the stress – time history during the impact process. Striking velocities up to 36 m/s were used. Response of the sapphire specimens to the impact was described using of the stress pulses recorded in the steel bar. The time development of the specimen damage was recorded using the high – speed photography. Stress pulses were evaluated both in the time as well as in the frequency domain. Experimentally recorded stress pulses have been compared with stress pulses corresponding to the elastic response of the specimen. These pulses have been obtained using the numerical simulation of the Taylor impact experiments .

**Key Word :** Sapphire; Taylor test ;stress pulse; spall fracture; crushing; frequency analysis;;numerical simulation

---

Date of Submission: 03-09-2024

Date of acceptance: 16-09-2024

---

### I. INTRODUCTION.

Sapphire (single crystal of  $\text{Al}_2\text{O}_3$ ) is widely used in many industries due to its superior physical, chemical and mechanical properties [1]. There are also application where the sapphire is subjected to very intensive loading. One of the example is the use of sapphire as the material of a hard front layer in transparent armor [2, 3]. There are many experimental techniques which are used for the investigation of brittle materials behaviour at strain rates corresponding to the loading process corresponding to the ballistic attack. The experimental research of the sapphire behaviour at high strain rates up to  $10^4 \text{ s}^{-1}$  is mostly based on the use of Split Hopkinson Pressure Bar (SHPB) method [4]. The response of the sapphire and other brittle materials to very intensive shock loading is studied using the experimental technique known as plate impact, which involves loading material in a state of one-dimensional (1D) strain at rates in the range  $10^5 - 10^7 \text{ s}^{-1}$  [5,6].

The strain and fracture behavior of materials at strain rates up to  $10^5 \text{ s}^{-1}$  is studied using the Taylor impact test. In this test, a cylinder made from tested material is launched against a rigid anvil. This test was originally proposed for the testing of metallic (ductile) materials when the output of this experiment is the deformed shape of the impacted cylinder. The modification of this experimental arrangement was extended for the study of high strain rates behaviour of brittle materials [7- 9].

Response of sapphire rod to the impact was studied in [10] . In this paper the elastic response of the sapphire rod was considered. It corresponds to relatively small impact velocities.

In the given paper a serie of Taylor impact experiments are performed on sapphire rods at higher striking velocities up to 36 m/s when rod (specimen) damage occurs. Sapphire rods are fired against the steel bar which remain elastic. This arrangement enables to record a time history of the stress originated from the specimen impact. The detail analysis of these records both in the time and frequency domain were performed. The main features of the specimen damage during impacts was monitored by high speed photography. In order to describe the effect of the specimen damage on the recorded stress pulses the numerical analysis of the Taylor impact experiments under assumption of the pure elastic response of the specimen was performed using ANSYS LS DYNA software.

## II. EXPERIMENTAL DETAILS

Taylor tests have been performed with cylindrical specimens of the sapphire. Sapphire crystals were produced in Saint-Gobain Company. Diameter of the specimen was 5 mm and length 25 mm. Specimens have been impacted in c - direction. For c – oriented rod the mechanical properties of sapphire are given in the Table 1[11].

**Table 1: Mechanical properties of sapphire (parallel to c axis, temperature 25°C, quasi static loading).**

Density ( $\text{kgm}^{-3}$ )	3970
Young modulus E (GPa)	435
Shear modulus G (GPa)	175
Poisson ratio $\nu$	0.25-0.30
Biaxial flexural strength (GPa)	1035
Compressive strength (GPa)	1.97
Tensile strength (GPa)	0.432
Vickers Hardness (GPa) – 10 N	17.4
$K_{IC}$ ( $\text{MPam}^{1/2}$ )	4.5

The sapphire rods (specimens) were fired against to steel bar. The steel bar is 1000 mm in length and 15 mm in diameter. The bar deformation during the specimen impact is elastic. The elastic properties of steel are : E = 216 GPa,  $\nu= 0.33$ . The steel density is  $7850 \text{ kgm}^{-3}$  . Stress pulses recorded by the strain gauge at the middle of the steel bar have been evaluated both in the time and frequency domain. In order to obtain more information on the specimen behavior impacts themselves were monitored by high speed photography, using PHOTRON FASTCAM SA-Z type 2100K-M, Frame Rate 210000fps, Shutter Speed 1.00  $\mu\text{s}$  . In order to reach a reasonable contrast the specimens were colored. All experiments were performed at the room temperature 25C.

## III. RESULTS AND DISCUSSION

The sapphire rods striking velocities were : 6,9,13.5,18,21,25 ,27 and 36 m/s. In the Fig.1 the stress time histories reported on the steel bar are displayed.

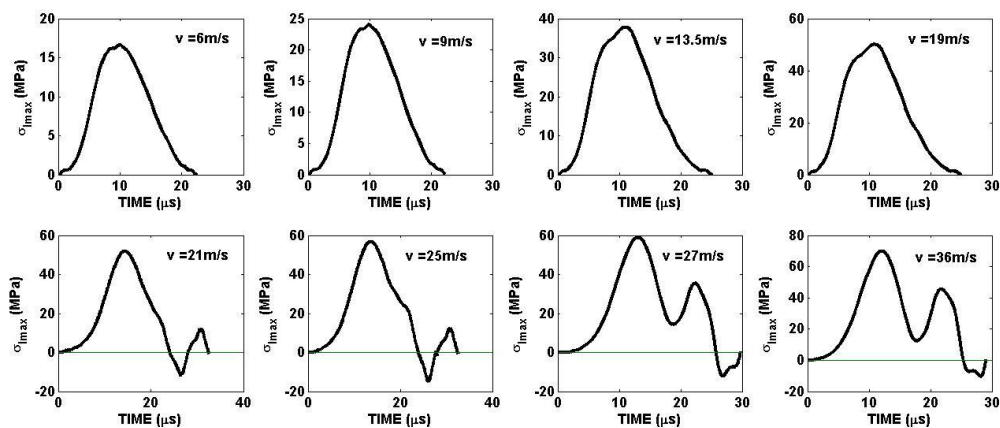


**Figure 1:Experimental records of the stress pulses  $\sigma_I(t)$**

The damage of the specimen starts at the striking velocity 9 m/s. The final specimen damage is shown in the Fig.2.

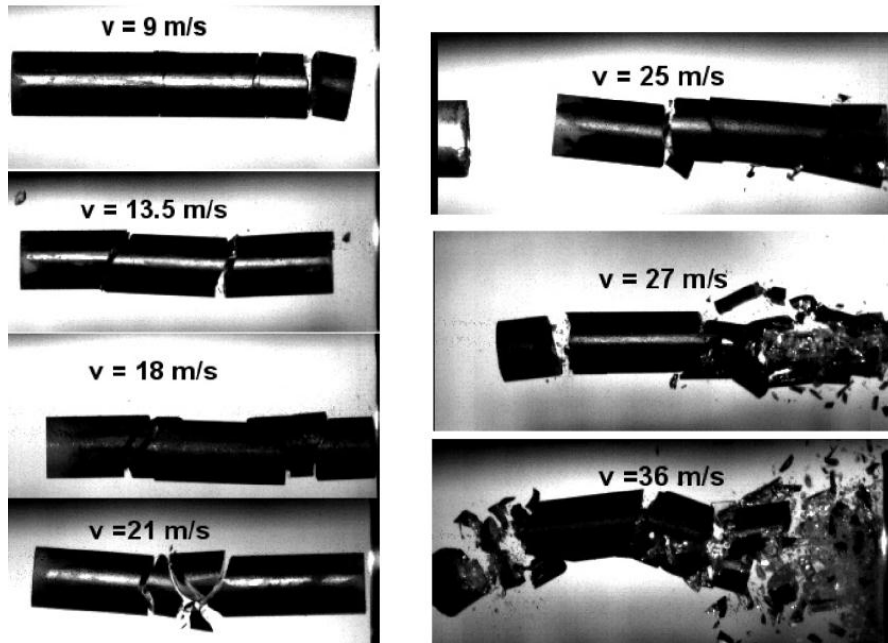


Figure 2: Resultant damage of the sapphire rod striking the steel bar

The damage of the sapphire rod at the striking velocity 9 m/s is in the form of multiply spall fracture. The details of the damage development is documented in the Fig.3.

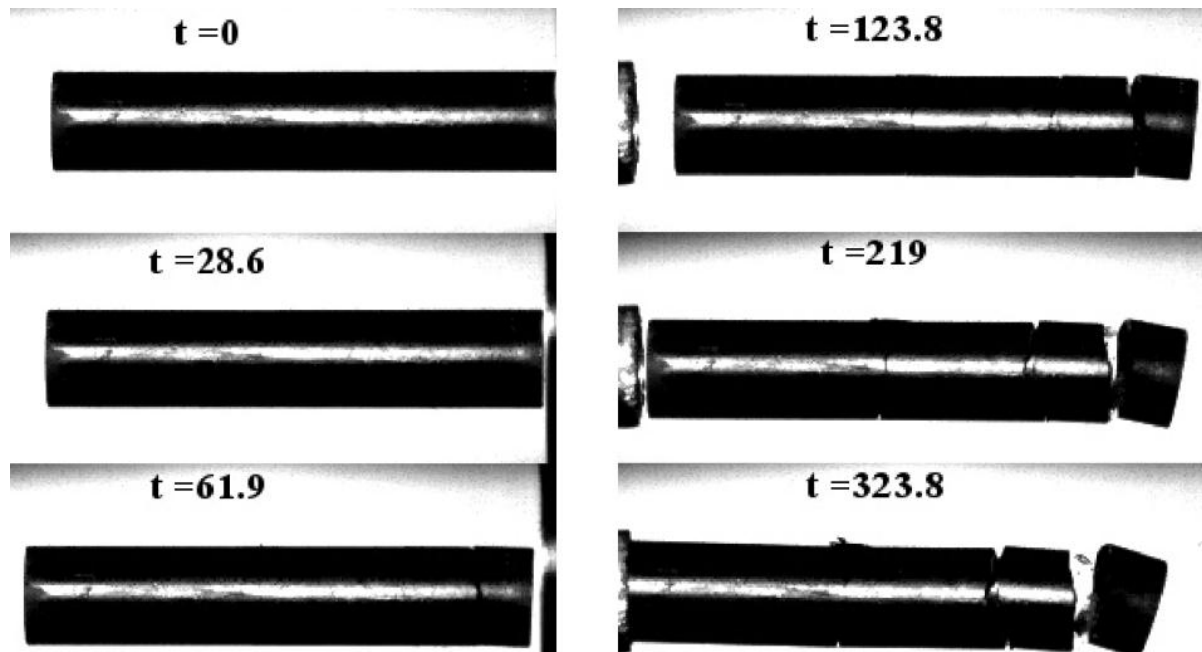


Figure 3: Specimen damage development in the glass specimen during the Taylor impact. The striking velocity was 9 m/s. The time  $t$  is given in  $\mu\text{s}$ .

Specimen moves from the left to the right. At the time about 23  $\mu\text{s}$  the specimen reflects from the steel bar. The damage of the specimen is in the form of multiply spall fracture. This fracture develops during the back movement of the specimen. The reflection of the sapphire rod from the steel bar is also observed for the striking velocity 13.5 m/s. The spall fracture occurs for all striking velocities. The increase in the striking velocity leads to the change of the spall fracture position. For highest used velocities the spall occurs near of the free end of the sapphire rod. At striking velocities 27 and 36 m/s the extensive fragmentation of the specimen is observed. Time history of the specimen damage development is documented in the Fig.4. The specimen damage begin in form of a crushing. After some time the spall fracture starts. Part of the specimen between spall “plane” and crushing zone

remains undamaged. The increase in the rod striking velocity to value  $v = 36$  m/s. leads to the significant extension in the crushing area - see Fig.5.

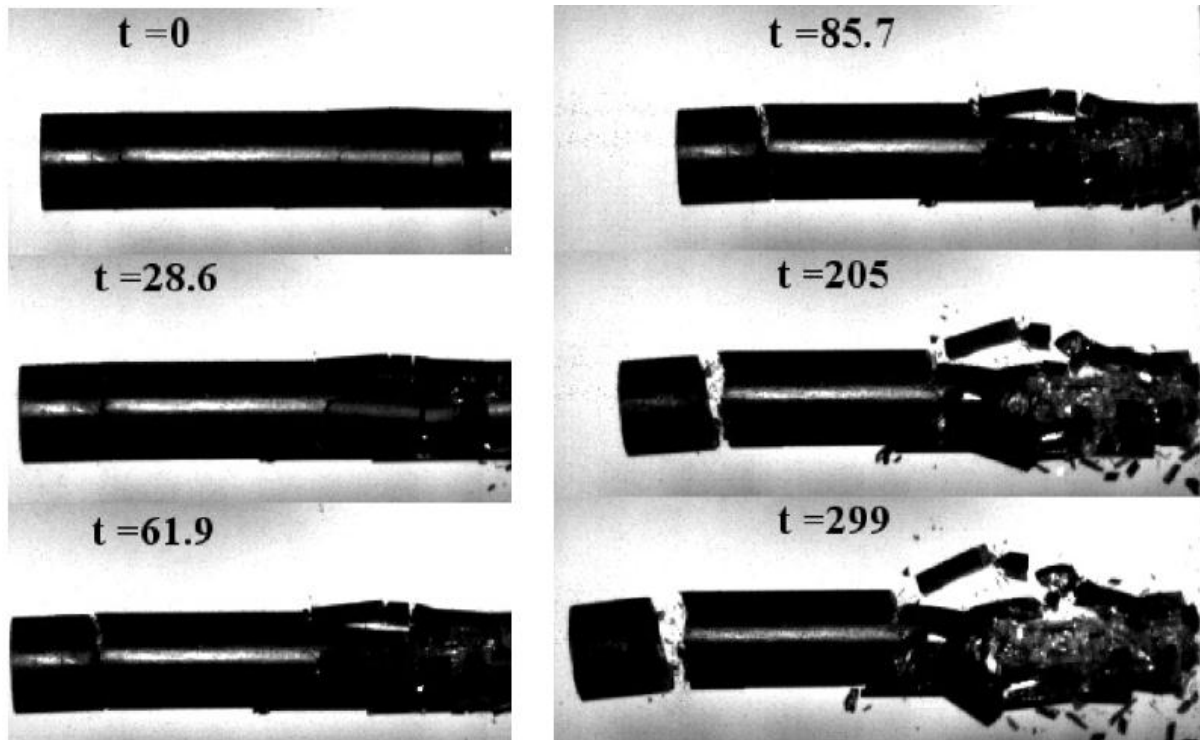


Figure 4: Development of the sapphire rod damage after impact on the steel bar. Striking velocity  $v = 27$  m/s. Time  $t$  is given in  $\mu$ s

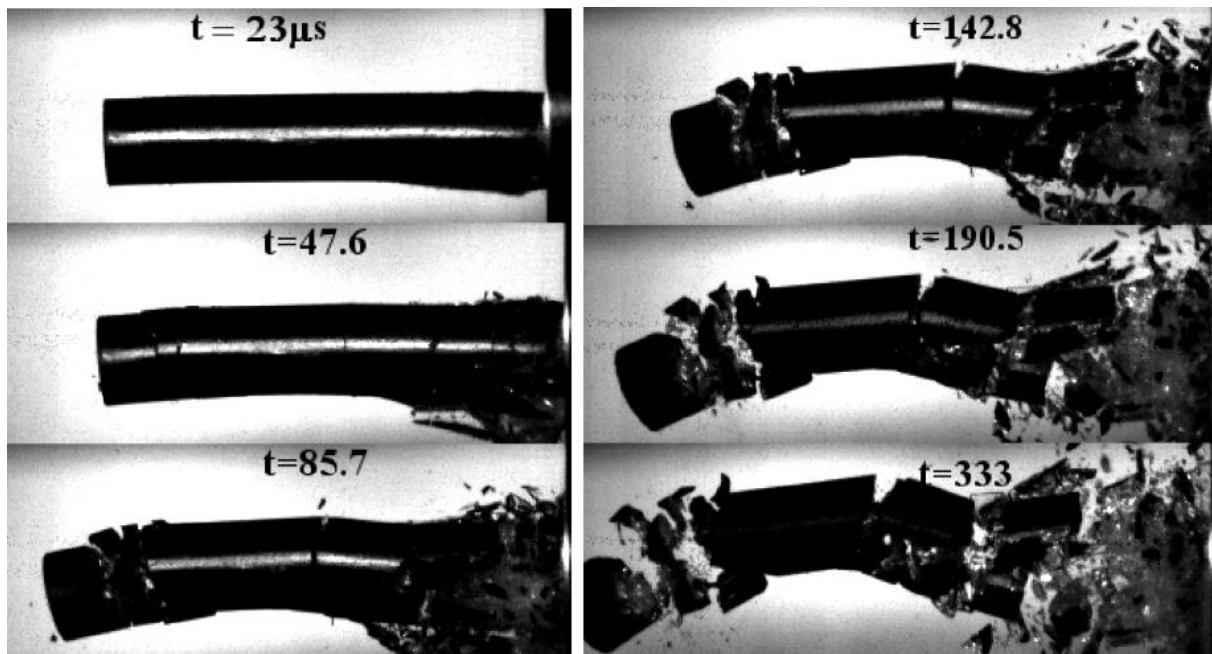


Figure 5: Development of the sapphire rod damage after impact on the steel bar. Striking velocity  $v = 36$  m/s. Time  $t$  is given in  $\mu$ s

Figure 6 illustrates two scanning electron microscopy (SEM) micrographs of fracture surfaces from test at striking velocity 18 m/s. It is clear from the fracture surfaces that cleavage controls the fracture down to the nano-scale.

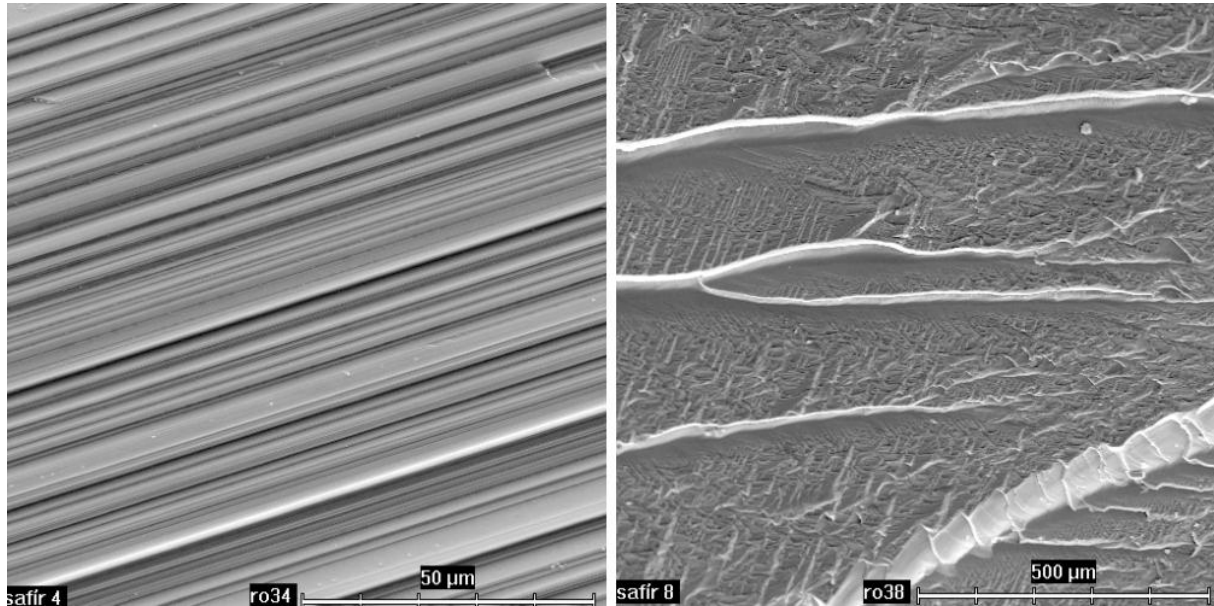


Figure 6: Two SEM micrographs of cleavage morphologies of fracture surfaces (Taylor test , striking velocity 18 m/s)

For higher striking velocity the fracture surfaces also exhibit cleavage morphology . Typical feature of the fracture surface is a river pattern [11] - see Fig.7. Similar results were obtained for the fracture surfaces of sapphire subjected to edge on impact. [12].

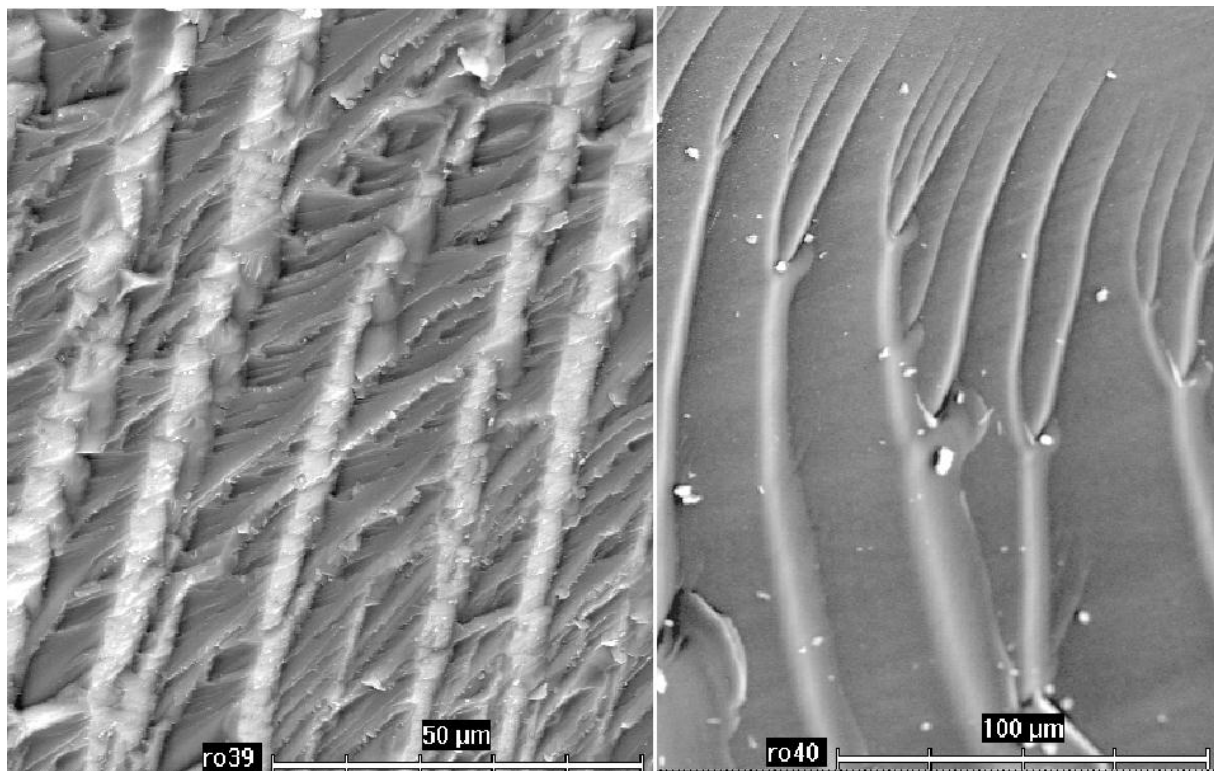
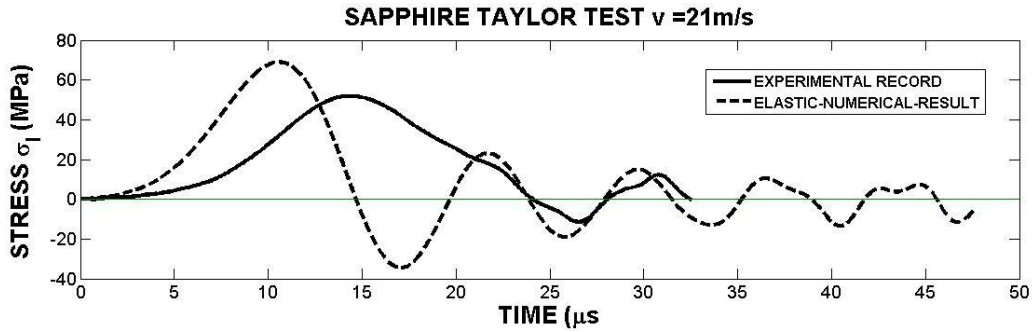


Figure 7: Two SEM micrographs of cleavage morphologies of fracture surfaces (Taylor test , striking velocity 25 m/s)

The development of the specimen damage affects the stress pulses  $\sigma_I(t)$  recorded in the steel (elastic) bar. In the Fig.8 an example of comparison between recorded stress pulse and stress pulse corresponding to purely elastic strain of the sapphire rod is presented. The stress pulses evaluated under assumption of pure elastic deformation were computed using LS DYNA finite element code.



**Figure 8: Comparison of stress pulse corresponding to the pure elastic response and stress pulse recorded during the Taylor test**

The damage leads to the decrease in the maximum of the stress pulse and to the increase in time when this maximum is reached. The same qualitative features were observed for all striking velocities.

The stress pulse,  $\sigma_1(t)$ , can be characterized by the following parameters :

- Maximum of the stress pulse (amplitude) :  $\sigma_{Im}$
- Impulse :  $I_t = \int \sigma_1(t) dt$
- Energy :  $w_t = \frac{1}{z_b} \int \sigma_1^2(t) dt$

In the Fig.9 the effect of the striking velocity  $v$  on the maximum stress  $\sigma_{Imax}$  is shown.

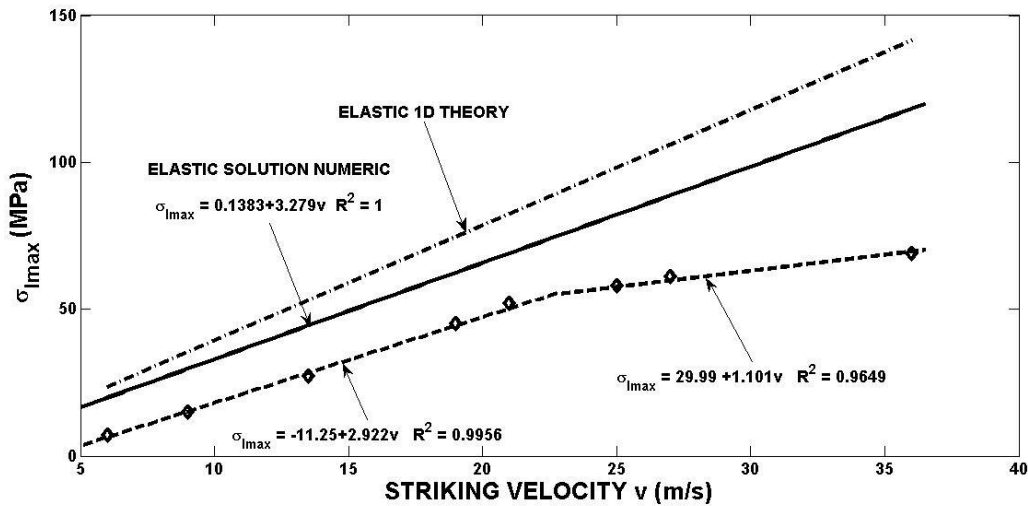


**Figure 9: Maximum of the stress vs. The rod striking velocity**

The experimental points ( symbol  $\diamond$ ) may be fitted by the bilinear function shown in the figure. The maxima lie below the values obtained by the numerical simulation of the Taylor test under assumption of elastic strain of the sapphire rod. Experimental points  $(v, \sigma_{Im})$  can be also compared with the values of obtained from the one dimensional (1D) theory of the elastic impact bar on bar. This theory is described e.g. in [13].The maximum of the stress pulse recorded in the elastic bar is given as :

$$\sigma_{Im} = \frac{\beta}{\beta+1} Z_b v \tag{1}$$

where  $\beta = \frac{A_s Z_s}{A_b Z_b}$ ,  $A$  is the cross section of the bar,  $Z$  is the acoustic impedance. Acoustic impedance is given

by product :  $Z = \rho c_0$ , where  $c_0$  is the bar velocity,  $c_0 = \sqrt{\frac{E}{\rho}}$ . Index  $s$  denotes the sapphire and index  $b$  corresponds to the elastic(steel) bar. For the values elastic constants given in the Table 1 this parameter reaches the value  $\beta = 0.1112$ . Acoustic impedance of the bar is  $Z_b = 41.18$  MPas/m. Using these data equation (1) can be written as :

$$\sigma_{Imax} = 4.121v \tag{2}$$

The use of the 1D theory of the rod elastic impact leads to the higher sensitivity of the maximum of the stress on the striking velocity in comparison with results of the numerical two dimensional solution.

Impulse and energy of the stress pulse  $\sigma_I(t)$  increase with the striking velocity  $v$  as shown in the Fig.10.

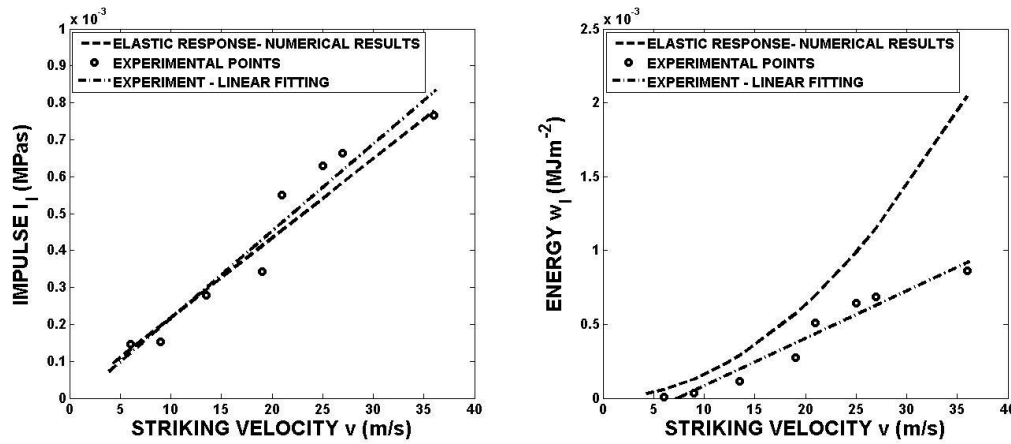


Figure 10: The effect of the striking velocity on the impulse and energy

Impulses and energies were evaluated both for the experimentally recorded stress pulses as well as for the stress pulses corresponding to the pure elastic response of the striking sapphire rod. The data can be fitted by the following functions :

Experimental records :

$$I_I = -2.014 \cdot 10^{-5} + 2.36 \cdot 10^{-5} \cdot v \quad R^2 = 0.9387 \quad (3a)$$

$$w_I = -0.0002369 + 0.00003211v \quad R^2 = 0.949 \quad (3b)$$

Elastic response of the specimen :

$$I_I = 2.321 \cdot 10^{-6} + 2.153 \cdot 10^{-5}v \quad R^2=1 \quad (4a)$$

$$w_I = -1.082 \cdot 10^{-6} + 2.894 \cdot 10^{-7}v + 1.569 \cdot 10^{-6}v^2 \quad R^2 = 1 \quad (4b)$$

Its evident that the specimen damage exhibits only small effect on the value of stress impulse. The development of this damage leads to significant decrease in the stress pulse energy.

The next information on the specimen response to the Taylor impact were evaluated also in the frequency domain. The result can be assessed using the integral transformation, when e.g. time function assigns its spectral function by means of [14]:

$$S(\omega) = \int_{-\infty}^{\infty} \sigma_I(t) e^{i\omega t} dt \quad (5)$$

where  $\omega=2\pi f$  is the angular frequency.

The spectral function is generally complex. It can be expressed as

$$S(\omega) = ReS(\omega) + ImS(\omega) = \sqrt{ReS(\omega)^2 + ImS(\omega)^2} e^{i\varphi} = Se^{i\varphi} \quad (6)$$

where  $S$  is the magnitude and  $\varphi$  the phase of the spectral function. Frequency dependencies of the magnitude and phase are displayed in the Figs.11-12.

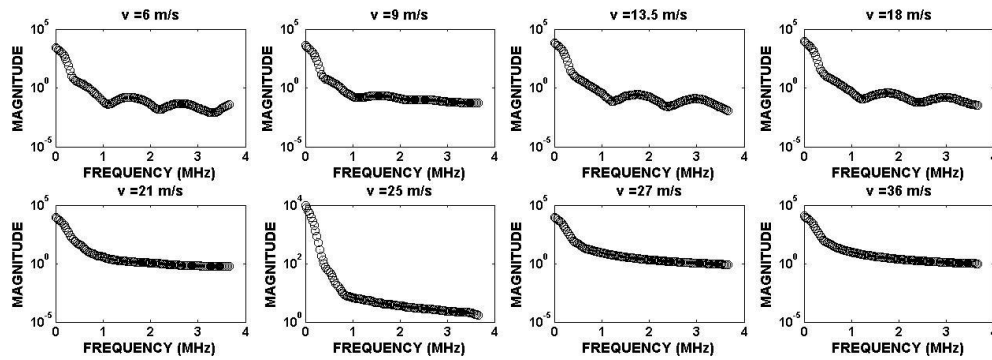


Figure 11: Magnitude of the spectral function

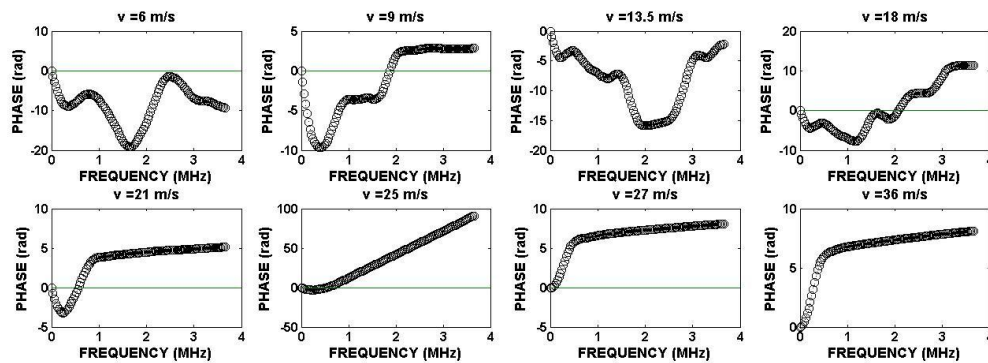


Figure 12: Phase of the spectral function

The magnitude significantly decreases with the frequency. The qualitative features of this dependence on the frequency are the same for all stress pulses. Some differences may be observed in the frequency dependences of the phase of the spectral functions. It is obvious that the main contribution to the frequency spectrum is focused in the narrow band at the zero frequency. The same is valid for the power spectrum density (PSD) which is distribution (over frequency) of the power contained in a signal (stress pulse) [14]. The units of the PSD are power (e.g. watts) per unit of frequency. This is documented in the Fig.13 where the PSD is plotted as the function of the frequency. In this figure the band where is concentrated 99% of the power is displayed. It is obvious that the width of this band increases with the striking velocity  $v$  i.e. with the increasing rod damage. From the spectral function some main characteristics can be also evaluated:

- The average amplitude  $\bar{P} = \frac{\sum_{i=0}^n P_i}{n+1}$

- The centroid of the frequency domain and the normalization average of the frequency domain:

$C_x = \frac{\sum_{i=0}^n P_i f_i}{\sum_{i=0}^n P_i}$      $C_y = \frac{\sum_{i=0}^n P_i f_i^2}{\sum_{i=0}^n P_i f_i}$  where  $P_i$  is the amplitude at the  $i$ -th frequency,  $f_i$ , in the frequency domain. The frequency dependence of these quantities are shown in the Fig.14. In this figure the frequency dependence of the average power (PSD) is also displayed. These quantities are compared with those obtained for the stress pulse computed for the elastic response of the sapphire rods during its striking with elastic (steel) bar. It is obvious that the highest difference is between normalized frequencies ( $C_y$ ).

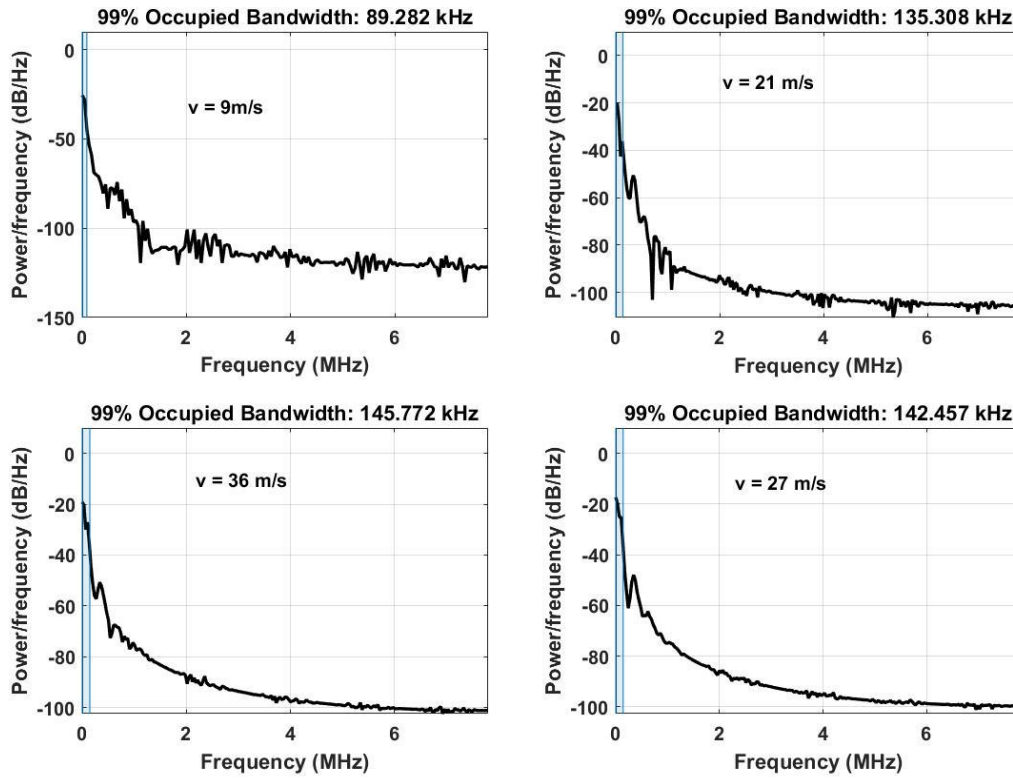


Figure 13: The power spectral density of the recorded stress pulses

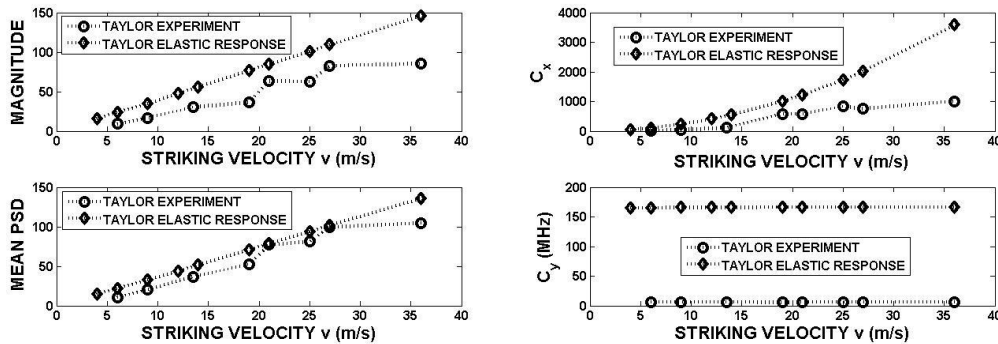


Figure 14: Main characteristics of the spectral functions. Magnitude represents the average value

The development of the specimen damage during its impact on the steel bar may be characterized by the increase in the bandwidth where the main part of the pulse power occurs. Also remaining parameters given by the Frequency analysis can be used for the description of the specimen behaviour during the Taylor test.

#### IV. CONCLUSIONS

The sapphire specimens behavior at the Taylor impact was studied up to the striking velocity 36 m/s. Experiments show that the shape of the stress pulses recording in the elastic (Hopkinson test) bar is strongly influenced by the specimen damage development. The high – speed camera results show that the specimen damage begins in form of spall fracture. The fracture surfaces exhibit cleavage form. This damage starts after reflection of the specimen from the steel bar. Increase in the specimen striking velocity leads to the fracture of the leading part of the specimen in form of fragmentation.

The maximum value (amplitude) of this pulse increases linearly with the striking velocity. This values of the amplitude lie below the amplitudes obtained for pure elastic response of sapphire rods during their impact

on the bar. These amplitudes were obtained using numerical simulation of the Taylor test experiment. Their values lie below the values predicted by the a simple one elastic dimensional theory (1D) of the specimen – bar impact. The changes in the stress pulse can be described using some other parameters of the stress pulse like impulse and energy. These changes may be also described in the frequency domain using the main characteristics of the pulse power spectrum obtained by the Fourier transform.

**Acknowledgements:** This research was supported by the European Regional Development Fund under Grant No. CZ.02.1.01/0.0/0.0/15\_003/0000493 (Centre of Excellence for Nonlinear Dynamic Behavior of Advanced Materials in Engineering).

## REFERENCES

- [1]. Dobrovinskaya, LA, Lytvynov, RA, Pishchik V. Sapphire: Material, Manufacturing, Applications, 2009.
- [2]. Jones C.D., J.B. Rioux, J.W. Locher, H.E. Bates, S.A. Zanella, V. Pluen and M. Mandelartz. Large-Area Sapphire for Transparent Armor, American Ceramic Society Bulletin 2006;85(3): 24-26
- [3]. Jones, C.D., J.B. Rioux, J.W. Locher, H.E. Bates, S.A. Zanella, V. Pluen and M. Mandelartz. “Ballistic Performance of Commercially Available Saint-Gobain Sapphire Transparent Armor Composites”, Advances in Ceramic Armor III, Ceramic Engineering and Science Proceedings. 2008; 28(5): 113-124.
- [4]. Feng Jiang, Xiasheng Luan, Ningchang Wang, Xipeng Xu, Xizhao La, Qiuling Wen. Research on dynamic mechanical properties of C-plane sapphire under impact loading. Ceramics International .2018;44: 9839-9847.
- [5]. Reinhart W.D., Chhabildas L.C., Vogler T.J. Investigation of phase transition and strength in single crystals sapphire using shock – reshock loading techniques. International Journal of Impact Engineering .2006;33: 655-669.
- [6]. Kleiner G.J., Chhabildas L.C., Reinhart W.D. Comparison of dynamic compression behaviour of single crystal sapphire to polycrystalline alumina. International Journal of Impact Engineering. 2011;38 : 473-479.
- [7]. Murray, N.H. N. K. Bourne, J. E. Field, Z. Rosenberg. Symmetrical Taylor Impact of Glass bars. AIP Conference Proceedings 1998;429- 533 (1998); <https://doi.org/10.1063/1.55560>
- [8]. Willmott, G.R.; Radford, D.D.; Taylor impact of glass rods, J. Appl. Phys. 2005;97:93522.
- [9]. Chhabildas, L.C.; Reinhart, W.D.; Dandekar, D.P.; Taylor impact experiments for brittle ceramic materials, Proc. of the Ceramic Armor Materials by Design, McCauley, J.W.; Crowson, A.; Gooch Jr., W.A.; Rajendran, A.M.; Bless, S.J.; Logan, K.V.; Normandia, M.; Wax, S. (Eds.), pp. 269-278; Publ. The American Ceramic Society, Westerville, OH, 2002.
- [10]. Xiaosheng Luana , Feng Jianga, Ningchang Wanga , Xipeng Xua, Xizhao Luc , Qiuling Wen. The mechanical response characteristics of sapphire under dynamic and quasi-static indentation loading. Ceramics International 2018;44: 15208 – 15218.
- [11]. Strassburger E., Patel P., Mc Cawley J.W. Visualization and Analysis of Impact Damage in Sapphire. Proceedings of the 26th International Symposium on Ballistics, Miami, FL, 12–16 September 2011.
- [12]. Rao L., Narayanamurthy V., Simha K.R.Y. ,2016. Applied Impact Mechanics. John Wiley and Sons, Ltd. Chichester, West Sussex, U.K. ISBN : 978-11-1924-180-5.
- [13]. Stoica P. and Moses R.: Introduction to Spectral Analysis, Prentice Hall, Upper Saddle River, NJ (1997).